Eur. Phys. J. B **10**, 29–34 (1999)

THE EUROPEAN PHYSICAL JOURNAL B

EDP Sciences

SANS structural determination of a nonionic surfactant layer adsorbed on clay particles

I. Grillo[1,a], P. Levitz[2], and Th. Zemb[1]

[1] CEA Saclay, Service de Chimie Moléculaire, bâtiment 125, 91191 Gif-sur-Yvette, France
[2] CRMD, CNRS, 1bis rue de la Ferollerie, 45071 Orléans, France

Received 4 August 1998

Abstract. We study adsorption of two nonionic surfactants ($C_{12}E_5$ and $C_{12}E_8$) on a dispersed suspension of negatively charged laponite particles. First, we quantify adsorption, *i.e.* the amount of adsorbed molecules per gram of dried solid. Then, we show that contrast variation experiments under controlled conditions along the adsorption isotherm of the surfactant on dispersed laponite particles allow to determine the average thickness of a nonionic surfactant layer adsorbed on a solid anisotropic particle.

PACS. 61.80.Hg Neutron radiation effects – 68.10.Jy Kinetics (evaporation, adsorption, condensation, catalysis, etc.)

1 Introduction

Reversible adsorption of nonionic surfactant such as polyethylene glycol alkyl ether or cationic surfactant on minerals is a known phenomenon [1–4]. Isotherms quantify adsorption rate, coverage, area per surfactant compared to inorganic lattice size. Their patterns involve free transfer energies of surfactant from bulk liquid phase to solid/liquid interface. However, they do not give direct information on the distribution of molecules at the solid/liquid interface. Surface aggregation, as well as continuous or discontinuous adsorption layer have been proposed for the adsorbed films [1,2,5–8]. The structural knowledge of particle coating is crucial to understand the stability of ternary systems made of surfactant, mineral particles and water.

Our aim in the experiment described here, is to measure the scattering produced only by the adsorbed layer, separated as much as possible from all other sources of scattering due to colloidal heterogeneities present in this mixed fluid. Since the samples are complex colloidal solutions made of water, counter-ions, surfactant molecules, anisotropic charged particles, X-Ray and neutron scattering are powerful methods to analyse shapes and relative position of colloidal structure [9]. Moreover, contrast variation in Small Angle Neutron Scattering (SANS) allows in principle to isolate the signal of adsorbed molecules from total scattering by matching particles with partial deuteration of the solvent.

The main prerequisite is to handle solid particles with simple and relatively well defined anisotropic shape. In this respect, we used Laponite RD, a synthetic anionic trioctaedric hectorite manufactured by Laporte. General composition is $Si_8Mg_{5.45}Li_{0.4}H_4O_{24}Na_{0.7}$. The particle shape is sufficiently well defined and may be correctly described as disks of 30 nm diameter and 1 nm thickness. Density is 2.65 cm^3/g. The particle form factor is correctly reproduced using the scattering intensity of randomly oriented short cylinders [10,11]. Anisotropic and flat particles are well suited to study adsorption processes due to the large available plane surface. We focus on adsorption of two nonionic surfactants: pentaethylene glycol monododecyl ether ($C_{12}E_5$) is obtained from Nikko (Japan) and octaethylene glycol monododecyl ether ($C_{12}E_8$) is purchased from Fluka. Phase diagram and physical properties are described by Strey [12] and Mitchell [13]. These surfactants form micelles at low concentration (< 1wt%) and swollen lamellar phases in water at higher concentrations.

The ideal experimental scattering situation is obtained when the number of micelles in the bulk is minimised with respect to the amount of surfactant adsorbed on clay particles in a single phase sample. To fulfil this condition, adsorption isotherms have to be measured prior to contrast variation experiments.

2 Adsorption isotherms

Laponite concentrations (S/L), defined as the mass of dried solid divided by the mass of aqueous solution are 0.2, 0.5 and 0.7%, well below the sol/gel transition [11]. pH of solutions are adjusted to 9 by addition of NaOH to avoid congruent dissolution of particles. A mother solution is prepared by addition of 10^{-1} mol/l of surfactant (25 times lower than the concentration of apparition

[a] e-mail: grillo@ill.fr

of the lamellar phase) in the clay solution at the chosen concentration S/L. The next samples are obtained by dilution of the mother solution in the clay solution. For a given S/L, initial surfactant concentrations ($c_{\rm ini}$) vary between 10^{-4} and 10^{-1} mol/l. After stirring and equilibration, clear and stable liquid suspensions are obtained. The problem is to separate surfactant monomers and micelles in the bulk from adsorbed surfactant. Laponite are small anionic particles and suspensions are stabilised by long-range electrostatic repulsions. Thus, adding salt reduces the screening length and flocculation of particles appears for an ionic strength of 2×10^{-2} mol/l [11]. At this low level of ionic strength, cmc measurements of $C_{12}E_5$ at pH = 9 either in pure water or in brine (2×10^{-2} mol/l of KBr) show that the cmc is not affected by the addition of salt and remains equal to 8×10^{-5} mol/l. Former studies in other solids such as silica or kaolinite particles have shown that ionic strength influences on the same order of magnitude the adsorption isotherm and the cmc [2,3]. Invariance of the cmc with ionic strength allows us to consider, as first approximation, that adsorption process is not affected by addition of 2×10^{-2} mol/l of KBr. After addition of KBr, samples are centrifuged at 4000 rpm for 12 hours. The equilibrium concentration of surfactant ($c_{\rm eq}$) is measured by a TOC (Total Organic Carbon) method in the supernatant. The amount of adsorbed surfactant Γ is calculated from the difference between initial and equilibrium concentrations of surfactant and divided by the mass of the dried solid. Influence of floculation is checked by preparing solutions of surfactant with 2×10^{-2} mol/l KBr before laponite addition. Flocculation and adsorption occur in parallel. However, TOC dosages of supernatant give the same adsorption values as the first preparation method, where adsorption on individual particles precedes floculation.

Figure 1 shows adsorption isotherms at room temperature of both $C_{12}E_5$ and $C_{12}E_8$ for different S/L. Adsorption Γ, in mole of surfactant per gram of dried solid, is plotted against the relative concentration $c_{\rm eq}$/cmc. Adsorption is independent of S/L. Isotherms have a sigmoidal shape and reach a plateau around the cmc ($c_{\rm eq}$/cmc ≈ 1). Such a behaviour has already been observed and predicted for $C_{12}E_6$ and $C_{12}E_8$ on hydrophilic silica [1,2,5,8]. When the polar chain length increases from 5 to 8 ethoxy groups, the plateau decreases from 4.2×10^{-3} mol/g to 1.9×10^{-3} mol/g and the adsorption isotherm shifts to lower value of relative concentration. Therefore adsorption occurs by the polar part of the adsorbed surfactant. Two possible interactions between polar chain and laponite surface can be considered: firstly, a hydrogen bounding between ethoxy groups and OH groups located inside the basal hexagonal cavities of the particles; secondly, dipolar interactions between polar chains of the adsorbed molecules and anionic charges located inside the particles. In any case, the interaction during the transfer from the bulk to the solid/water interface has to be seen as an exchange mechanism involving adsorbed water. The mean consequence is a weak interaction with the solid surface and a rising part of the adsorption isotherm below but near the cmc.

Table 1. Neutron scattering parameters: length scattering density.

	ρ (cm^{-2})
D_2O	6.38×10^{10}
H_2O	-5.59×10^{9}
laponite	3.94×10^{10}
$C_{12}E_5$	1.29×10^{9} *
	1.86×10^{9} **

* dehydrated surfactant

** hydrated surfactant in a 32.7 w% H_2O and 67.3 w% D_2O solvent

Adsorption isotherm plateaux are found around 4.2×10^{-3} and 1.9×10^{-3} mol/g for $C_{12}E_5$ and $C_{12}E_8$ respectively. It can be now interesting to calculate the apparent molecular section at the solid/liquid interface. Using the radius, thickness and particles density values defined in the introduction, the total specific surface $S_{\rm p}$ of a nude particle is around 800 m^2/g. Thus, the apparent molecular sections of $C_{12}E_5$ and $C_{12}E_8$ are respectively 32 Å^2 and 70 Å^2. As a comparison, adsorption at the silica/water interface gives 35 Å^2 and 55 Å^2 for $C_{12}E_5$ and $C_{12}E_8$ [1], *i.e.* a globally more compact adsorption layer.

In order to get a geometrical parameter concerning the adsorption layer structure, two possible reference states may be considered: either the surfactant monolayer at the water/air interface or the bilayer of lamellar phase in bulk water. For the first one, surface tension γ of surfactant, plotted against $\ln(c)$ yields to a the linear function below the cmc. The slope is related to the Gibbs surface excess from which molecular area and specific surface are calculated. One find 47 and 70 Å^2/molecule for $C_{12}E_5$ and $C_{12}E_8$ respectively, at the interface air/water. In the lamellar phase, the area per molecule is 46 Å for $C_{12}E_5$ and 78 Å for $C_{12}E_8$ [14]. These molecular sections $\sigma_{\rm s}$ do not change strongly between a liquid/liquid and an air/liquid interface. We can not assume for ground that the absorption layer at the solid/liquid interface is homogeneous. Formation of either monolayer or bilayer or finite surface aggregates are possible, below the critical micellar concentration (cmc). Nevertheless, we will define an apparent surface coverage c, in reference to the specific area in the lamellar phase. c reads to:

$$c = \frac{N\Gamma\sigma_{\rm s}}{S_{\rm p}} \qquad (1)$$

N is the Avogadro number. A complete surface bilayer, with no defects yields to $c = 2$. At the plateau of the adsorption isotherm, $c = 1.4$ for $C_{12}E_5$ and 1 for $C_{12}E_8$. These values demonstrate the possibility to form an incomplete bilayer on the mineral surface, in a large domain of concentrations between one and 10^2 cmc, where a large number of micelles is formed in the bulk.

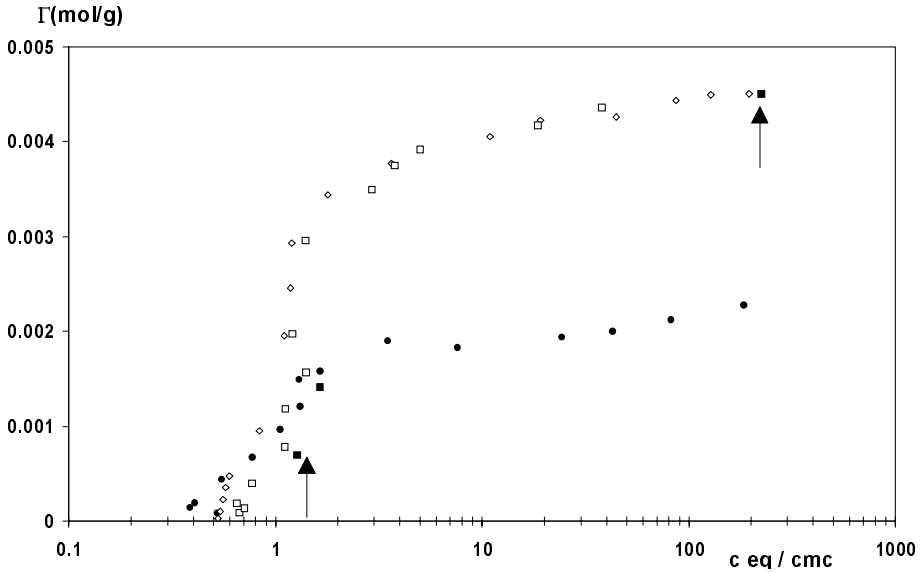

Fig. 1. Comparison of adsorption isotherm of $C_{12}E_5$ and $C_{12}E_8$ on laponite and influence of clay concentration (S/L, mass of dried clay divided by mass of brine) on adsorption. (●) $C_{12}E_8$ $S/L = 0.5\%$, (◇) $C_{12}E_5$ $S/L = 0.2\%$, (□) $C_{12}E_5$ $S/L = 0.5\%$, (■) $C_{12}E_5$ $S/L = 0.7\%$.

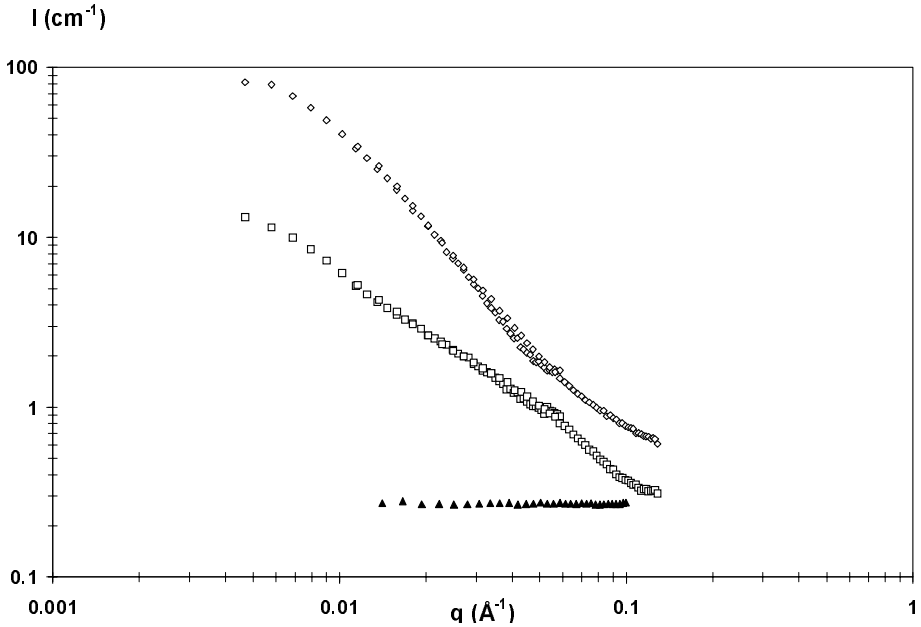

Fig. 2. Neutron scattering of solutions of pure laponite, $C_{12}E_5$ and laponite and micelles of $C_{12}E_5$, for one sample-detector distance, at two wavelengths. Spectra are plotted in log-log scale in absolute unit before subtraction of incoherent scattering. (▲) laponite $S/L = 0.7\%$ in deuterated solvent; (◇) laponite $S/L = 0.7\%$ and $C_{12}E_5$ for an initial concentration $c_{\rm ini} = 5 \times 10^{-2}$ mol/l corresponding to $c_{\rm eq} = 1.8 \times 10^{-2}$ mol/l; (□) micelles of $C_{12}E_5$, $c_{\rm eq} = 1.8 \times 10^{-2}$ mol/l.

3 Small angle neutron scattering

We focus now on $C_{12}E_5$. SANS experiments were performed on PAXE (LLB Saclay) at two wavelengths: 5.5 Å and 11 Å; sample-detector distance is 5 m; q-range is from 4.5×10^{-3} to 0.13 Å^{-1}. We calculate from Table 1 that the signal of laponite may be extinguished with 67.3 w% D_2O in H_2O. Scattering of pure laponite in this deutered solvent is flat and intensity equals 2×10^{-2} cm^{-1} (Fig. 2). This value of incoherent background is 10 to 100 times smaller than the intensity of micelles or complex fluid under investigation. Laponite is well matched. Contrast $\Delta\rho$ between dehydrated surfactant and solvent equals 3.8×10^{10} cm^{-2} and allows to get an exploitable signal/background ratio for acquisition times varying between 30 minutes and 2 hours depending on concentrations and wavelengths.

The equilibrium concentration for each initial surfactant concentration is deduced from the adsorption

isotherms shown in Figure 1. Experiments are carried out for one clay concentration $S/L = 0.7\%$, and two surfactant concentrations $c_{\rm ini} = 5\times10^{-2}$ (case a), 5×10^{-3} mol/l (case b). Our aim is to follow the evolution of the surfactant layer parameters: size, shape and amount. Corresponding points of isotherm are indicated by vertical arrows in Figure 1. For equilibrium concentrations ($c_{\rm eq}$) equal to 10^{-4} and 1.8×10^{-2} mol/l, adsorption is respectively 7×10^{-4} and 4.5×10^{-3} mol/g on the plateau.

For each sample, adsorbed surfactant signal is calculated as follows. We measure the scattering of a ternary sample with surfactant, laponite and water and the scattering of excess micelles and monomers without solid particles. Intensity is always calculated in absolute scale ($\rm cm^{-1}$). We work with sufficiently dilute systems to minimise the relative amount of micelles in excess in the bulk. Ratios between adsorbed and bulk surfactants are 2 and 50 for cases a and b respectively. The intensity of micelles is 10 times lower than the intensity of clay and surfactant (Fig. 2). Thus, we neglect crossed terms in the amplitude, in the calculation of the scattered intensity. The signal of adsorbed surfactant is isolated by subtraction of the contribution of the micelles from the total scattering, corrected from incoherent scattering.

4 Modelling

As shown in Figures 3 and 4, the spectra, plotted in log-log scale, reach a plateau for $q < 10^{-2}$ Å^{-1} proportional to the concentration of objects; the slopes are related to the object shape.

Clay particles are considered as monodisperse disks. For $S/L = 0.7\%$, average distances between clay particles is 800 Å. We suppose that there is no correlation between these diluted particles and hence $S(q) = 1$.

In these conditions, for unmatched naked particles, intensity per volume unit is:

$$\frac{I(q)}{V}(\rm cm^{-1}) = \frac{N_{\rm part}}{V}(\rho_{\rm c}-\rho_{\rm w})^2\langle A_{r,e}(\mathbf{q})A^*_{r,e}(\mathbf{q})\rangle \qquad (2)$$

$\rho_{\rm c}$ is the average length density of the laponite and $\rho_{\rm w}$ these of the solvent.

Brackets indicate average over θ, for randomly oriented particles, where θ is the angle between the normal to the disk and the wave vector q.

For disk of thickness $2e$ and radius r, the scattering amplitude $A_{r,\rm e}$ is [10]:

$$A_{r,\rm e}(\mathbf{q}) = \pi r^2 e\frac{\sin(q_z e)}{q_z e}\frac{2J_1(q_{xy}r)}{q_{xy}r} \qquad (3)$$

where $q_z = q\cos\theta$ and $q_{xy} = q\sin\theta$, J_1 is the first order Bessel function.

Taking $2e = 10$ Å and $r = 150$ Å for naked particles, experimental and calculated spectra have a good agreement between 10^{-2} and 0.4 Å^{-1} as shown in Figure 3 [11]. A plot of $\log(q)$ *versus* $\log(I)$ has a slope of -2, signature of bidimensional objects, in the range $2\times10^{-2} < q < 0.4$ Å^{-1}.

In deuterated solvent, for matched particles, Figure 3 shows that the scattering produced by the coated particles differs as expected from the one of the uncovered particles. The SANS signal reaches a plateau for $q < 10^{-2}$ Å^{-1}.

We have no information on the density profile in the adsorbed layer. As a first approximation, we assume that the particles are surrounded by an homogenous layer of surfactant of effective thickness $h_{\rm eff}$, perpendicular to the particles interface. Thus, the unknown total thickness h and profile $\Delta\rho(z)$ in the sample is replaced by a step function of an effective thickness $h_{\rm eff}$ and an average $\Delta\overline{\rho}$ calculated in comparison with the solvent (Fig. 5) in such a way that we keep constant the number of scatters:

$$\int_0^h {\rm d}z\Delta\rho(z) = \Delta\overline{\rho}h_{\rm eff}. \qquad (4)$$

Scattering amplitude for this layer of thickness $h_{\rm eff}$ is:

$$A_{\rm layer}(\mathbf{q}) = A_{r+h_{\rm eff},e+h_{\rm eff}}(\mathbf{q}) - A_{r,e}(\mathbf{q}) \qquad (5)$$

and scattered intensity per volume unit is:

$$\frac{I(q)}{V}(\rm cm^{-1}) = \frac{N_{\rm part}}{V}\Delta\overline{\rho}^2\langle A^*_{\rm layer}(\mathbf{q})A_{\rm layer}(\mathbf{q})\rangle \qquad (6)$$

$$\frac{I(q)}{V}(\rm cm^{-1}) = \frac{N_{\rm part}}{V}\Delta\overline{\rho}^2\int_0^{\pi/2}{\rm d}\theta\sin\theta \times\left\{\begin{array}{c}\pi(r+h_{\rm eff})^2(2e+2h_{\rm eff})\frac{\sin q_z(e+h_{\rm eff})}{q_z(e+h_{\rm eff})}\frac{2J_1q_{xy}(r+h_{\rm eff})}{q_{xy}(r+h_{\rm eff})}\\ -\pi r^2\ e\frac{\sin q_z e}{q_z e}\frac{2J_1q_{xy}r}{q_{xy}r}\end{array}\right\}^2. \qquad (7)$$

To run our calculation, we need the following input data:
- the adsorbed surfactant concentration Γ given by the isotherm in mol per unit of particle mass;
- the particle specific surface $S_{\rm p}$ (per unit of mass);
- the length scattering densities of the deutered solvent ($\rho_{\rm w}$) and the dehydrated surfactant molecules ($\rho_{\rm s}$) given in Table 1;
- the total volume of adsorbed dehydrated surfactant $v_{\rm surf}$ per unit of particle mass

The next step is to compute $\Delta\overline{\rho}$ in agreement with equation (4). Neglecting the edge effects (7% of the total surface of a solid particle), we can write:

$$\int_0^h {\rm d}z\Delta\rho(z) = h[\rho_{\rm w}(1-x)+x\rho_{\rm s}-\rho_{\rm w}] = hx[\rho_{\rm s}-\rho_{\rm w}] = \Delta\bar{\rho}h_{\rm eff}. \qquad (8)$$

x is the true surfactant volume fraction inside the adsorption layer and reads:

$$x = \frac{v_{\rm surf}}{S_{\rm p}h}\cdot \qquad (9)$$

In equation (8) as in Figure 5, we consider a constant scattering length density within the surfactant layer

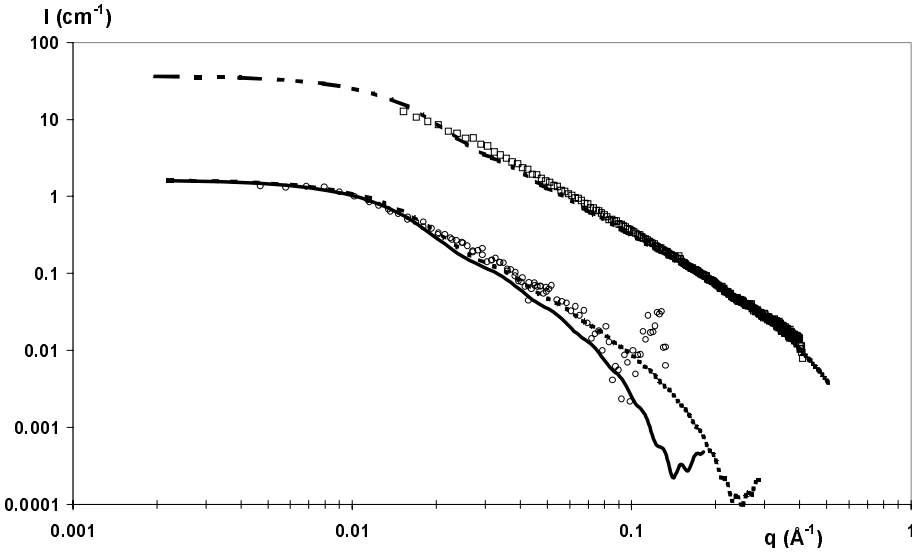

Fig. 3. Top curves: X-ray scattering of pure laponite in water: (□) $S/L = 0.7\%$, and simulated form factor (– - –) of an isolated particle. Bottom curves: Adsorption layer scattering of $C_{12}E_5$ on laponite 0.7% for one equilibrium concentration of 10^{-4} mol/l; symbols are experimental points, lines are calculated for different hypothesis of layer thickness and surfactant volume fractions: (—) $h_{\text{eff}} = 14$ Å and $x_{\text{eff}} = 0.24$, (- -) $h_{\text{eff}} = 3.7$ Å and $x_{\text{eff}} = 1$.

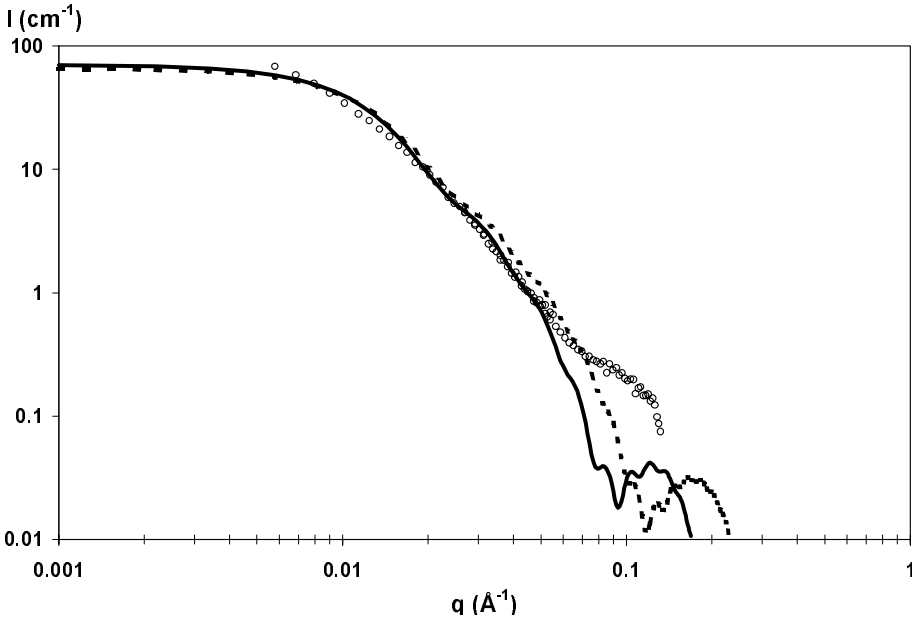

Fig. 4. Adsorption layer scattering of $C_{12}E_5$ on laponite 0.7% for one equilibrium concentration of 1.8×10^{-2} mol/l; symbols (O) are experimental points, lines are calculated for different hypothesis layer thickness and surfactant volume fractions: (—) $h_{\text{eff}} = 28$ Å and $x_{\text{eff}} = 0.62$, dotted line (- - -) $h_{\text{eff}} = 19$ Å and $x_{\text{eff}} = 1$.

and we assume that this value is the sum of nucleus densities by the molecular volume, deduced from solution density measurement. This approximation has been shown to be valid still $q = 0.4$ Å^{-1} for pure micelles [15] and is applied here for a q-range 0.01 Å$^{-1} < q < 0.4$ Å^{-1}.

From equations (8, 9), we get:

$$\Delta\bar{\rho} = \frac{v_{\text{surf}}}{S_{\text{p}} h_{\text{eff}}}(\rho_{\text{s}} - \rho_{\text{w}}). \tag{10}$$

The only adjustable parameter is the effective layer thickness h_{eff}. We introduce the effective volume fraction of surfactant inside the adsorption layer as:

$$x_{\text{eff}} = \frac{v_{\text{surf}}}{S_{\text{p}} h_{\text{eff}}} \geq x \quad \text{as} \quad h_{\text{eff}} \leq h. \tag{11}$$

The scattered intensity depends on the number of objects in solution and on the layer thickness h_{eff}; patterns and slopes vary with h_{eff}.

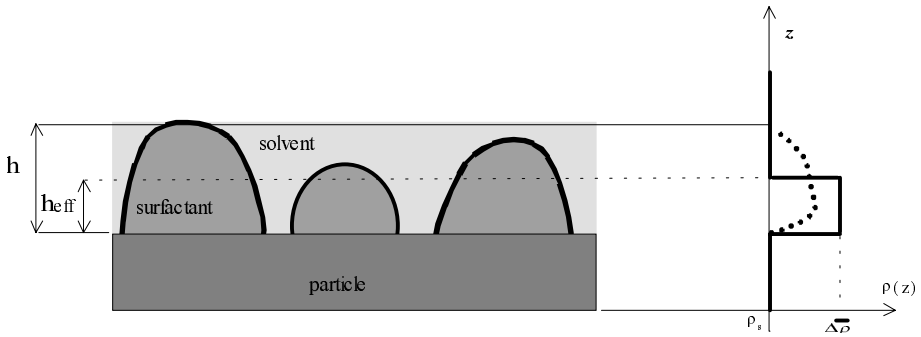

Fig. 5. Schematic picture of the incomplete surfactant layer of total thickness h, adsorbed on the solid surface. h_{eff} is the effective thickness. The unknown length density profile is replaced by a step profile, which keep constant the number of scatterers, according to equation (4).

5 Results and discussion

For an equilibrium concentration of 10^{-4} mol/l, close to the cmc (8×10^{-5} mol/l), the best fit is obtained with $h_{\text{eff}} = 3.7$ Å corresponding to $x_{\text{eff}} = 1$. For 1.8×10^{-2} mol/l, $h_{\text{eff}} = 28$ Å (thickness of a bilayer in the lamellar phase), $x_{\text{eff}} = 0.62$. A similar value of the water volume fraction x_{eff} is found in the outer layer of a direct micelle, usually designed as "polar layer". This could be determined only using the large q, $0.2 < q < 0.6$ Å^{-1} of SANS spectra [15].

At low coverage, the effective layer thickness is lower than the length of one molecule of surfactant. For high coverage, the thickness layer is the length of two molecules, with a compactness $x_{\text{eff}} < 1$. Thus, the real compactness is less than one and evidences the existence of either an incomplete bilayer or an aggregative adsorption layer.

Best fits are obtained for $q < 8 \times 10^{-2}$ Å^{-1}. For larger q, intensities are very faint, about 5×10^{-2} cm^{-1} and it is difficult to extract signal from background. If aggregation in the form of surface clusters would be significant, average distances between aggregates on the solid surface would be 50 Å. Thus, the correlation peak would appear at $q = 10^{-1}$ Å^{-1}. With the resolution used ($q_{\max} = 1.5 \times 10^{-1}$ Å^{-1}) and available flux (about 10000 n s^{-1} cm^{-2} for $\lambda = 5.5$ Å), the detailed picture of the incomplete layer including the in-planer correlation term, cannot be detected.

This SANS contrast variation experiments give a direct observation of adsorbed nonionic surfactants on a mineral surface in solution. In the present experiment, we demonstrate the existence of a globally incomplete bilayer of average thickness 30 Å, where the surfactant molecules are adsorbed by the polar part.

In the case of $C_{12}E_6$, specular neutron scattering experiments, performed on flat silica surface [5,7], agree with our conclusion. However such an approach cannot be extended to the case of colloïdal particles. The origin of the "incomplete bilayer" or in other words, a collection of "surface aggregates" certainly involved the specific nature of the surfactant polar head (POE). This one has a similar or a more larger volume than the alkyl chain. Near the particle surface, a POE chain can "explore" the surface and sticks to it, in different ways. Weak interaction between POE chain and solid particle allow to rebuilt finite and curved surfactant aggregates onto the solid/liquid interface, below but close to the cmc. Interesting enough, adsorption of cationic surfactant (CTAB) on laponite particle [4,6,7] starts well below the cmc and first involves a cation-exchange. Lateral interactions between alkyl chains (the so called hydrophobic effect) induce a condensation of the ionic head close to the particle surface and the appearance of extended 2-D aggregates such as a monolayer or an almost complete bilayer.

It is a pleasure to thank J. Teixera for his kind hospitality at the Laboratoire Léon Brillouin.

References

1. P. Levitz, Langmuir **7**, 1595-1608 (1991).
2. S. Partyka, S. Zaini, M. Lindheimer, B. Brun, Coll. Surf. **12**, 255-270 (1984).
3. R. Denoyel, Thèse de docteur es-sciences, Université de Provence Aix-Marseille I, France (1987).
4. B. Brahimi, P. Labbe, G. Reverdy, Langmuir **8**, 1908-1918 (1992).
5. E.M. Lee, R.K. Thomas, P.G. Cummins, E.J. Staples, J. Penfold, A.R. Rennie, Chem. Phys. Lett. **162**, 196-202 (1989).
6. H.J.M. Hanley, C.D. Muzny, B.D. Butler, Langmuir **13**, 5276-5282 (1997).
7. J. Penfold, E.J. Staples, I. Tucker, L.J. Thompson, Langmuir **13**, 6638-6643 (1997).
8. V.L. Alexeev, P. Ilekti, J. Persello, J. Lambard, T. Gulik, B. Cabane, Langmuir **13**, 2392-2401 (1996).
9. P. Lindner, Th. Zemb, *Neutron, X-Ray and Light Scattering: introduction to an investigative tool for colloidal and polymeric systems*, edited by P. Lindner, Th. Zemb (North-Holland Delta Series, 1991).
10. A. Guinier, G. Fournet, *Small Angle Scattering of X-Rays* (Wiley: New York, 1955).
11. A. Mourchid, A. Delville, J. Lambard, E. Lécolier, P. Levitz, Langmuir **11**, 1942-1950 (1995).
12. R. Strey, R. Schömacker, D. Roux, F. Nallet, U. Olsson, J. Chem Soc, Faraday Trans. **86**, 2253-2261 (1990).
13. D.J. Mitchell, G.J.T. Tiddy, L. Waring, T. Bostok, P. McDonald, J. Chem Soc, Faraday Trans. 1 **79**, 975-1000 (1983).
14. T. Sottmann, R. Strey, S.-H. Chen, J. Chem. Phys. **106**, 6483-6491 (1997).
15. B. Cabane, Th. Zemb, Nature **314**, 305 (1985).